

**CIRCULATION COPY  
SUBJECT TO RECALL  
IN TWO WEEKS**

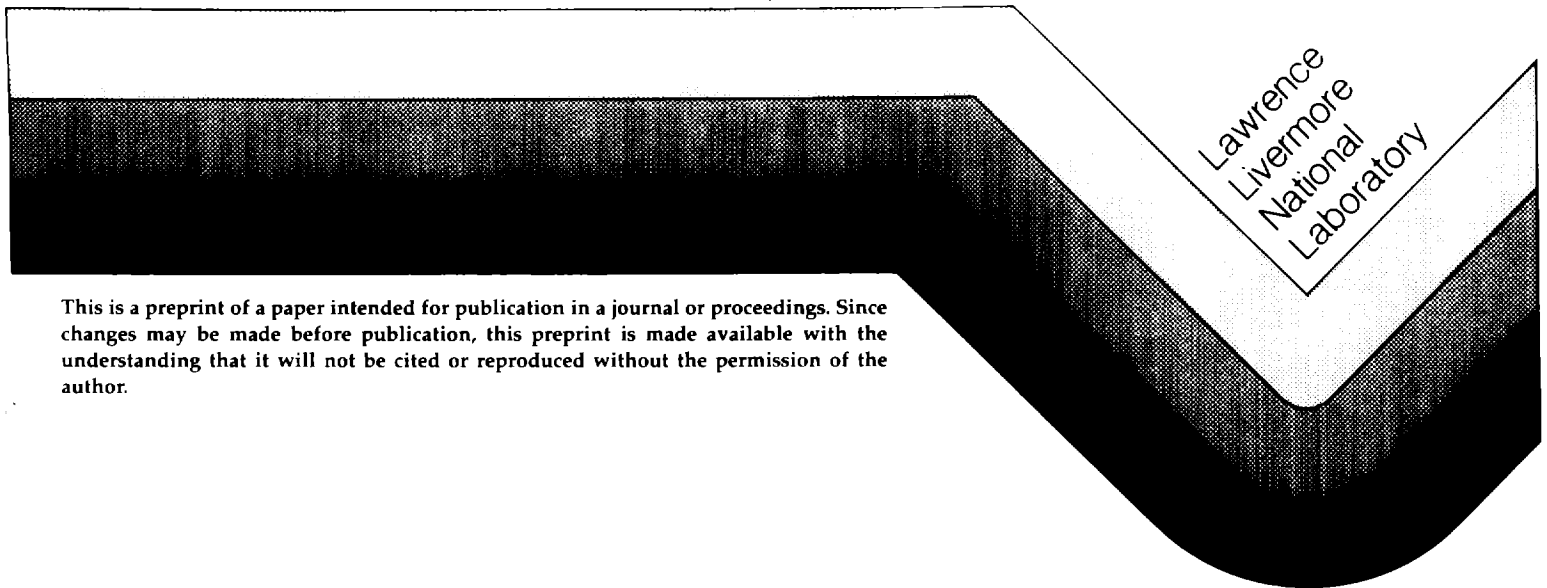
**UCRL- 92489  
PREPRINT**

**FURTHER DEVELOPMENT OF A GENERAL-PURPOSE, PACKED-BED MODEL  
FOR ANALYSIS OF UNDERGROUND COAL GASIFICATION PROCESSES**

**C. B. Thorsness  
S.-W. Kang**

This paper was prepared for submittal to the:  
11th Annual Underground Coal Gasification  
Symposium, Denver, CO, August 11-14, 1985.

August 1985



This is a preprint of a paper intended for publication in a journal or proceedings. Since changes may be made before publication, this preprint is made available with the understanding that it will not be cited or reproduced without the permission of the author.



#### DISCLAIMER

This document was prepared as an account of work sponsored by an agency of the United States Government. Neither the United States Government nor the University of California nor any of their employees, makes any warranty, express or implied, or assumes any legal liability or responsibility for the accuracy, completeness, or usefulness of any information, apparatus, product, or process disclosed, or represents that its use would not infringe privately owned rights. Reference herein to any specific commercial products, process, or service by trade name, trademark, manufacturer, or otherwise, does not necessarily constitute or imply its endorsement, recommendation, or favoring by the United States Government or the University of California. The views and opinions of authors expressed herein do not necessarily state or reflect those of the United States Government or the University of California, and shall not be used for advertising or product endorsement purposes.

FURTHER DEVELOPMENT OF A GENERAL-PURPOSE, PACKED-BED MODEL  
FOR ANALYSIS OF UNDERGROUND COAL GASIFICATION PROCESSES

by

C. B. Thorsness 1/  
S.-W. Kang 1/

---

ABSTRACT

Further development of a theoretical modeling analysis for characterizing reacting flows through packed beds is presented. These flows are related to the underground coal gasification conditions in terms of combustion and multi-component chemical reactions taking place inside charring coal beds. Time-dependent, two-dimensional (including axisymmetrical) partial differential equations (PDE's) describing conservation of mass, species, momentum, and the thermal energy are formulated. These PDE's are then recast into a set of ordinary differential equations (ODE's) with time the independent variable. The resulting ODE's are solved by applying a method-of-lines (MOL) technique. The present formulation considers: the transport phenomena at the wall; various transient flow cases; reactions of gas and solid species; a wide range of options on the boundary conditions; temperature-dependent physical parameters; and rezoning capabilities. A numerical code called GSF has been developed, and computer runs have been performed to verify various aspects of the physical models as well as the numerical approach taken in the present analysis. These include favorable agreements with available analytical solutions for simple, one-dimensional flows and two-dimensional non-isotropic heat transfer to a wall. For more complicated flow situations for which there are no analytical solutions, good agreements between the results of the present method and those of alternative numerical methods have also been obtained.

INTRODUCTION

During underground coal gasification (UCG) a significant portion of the process can take place in a packed bed, inside which the flowing gas interacts with solid particles. A variety of mechanisms are involved: (1) reactants in the gas phase move to the particle surfaces and react with them, and products then move back into the gas stream; (2) purely gas-phase reactions may occur when combustible gas comes in contact with injected oxygen; (3) heat

energy within the bed moves from hotter zones to cooler ones (e.g., from combustion zones to wall areas). Thus understanding of the UCG process is enhanced by analyzing the packed-bed processes to see how such parameters as gas composition and coal consumption are affected by changes occurring in this portion of the underground system.

The aim of this work is to develop a mathematical model of the packed bed geometry embodied in a numerical

---

1/ Lawrence Livermore National Laboratory, Livermore, CA 94550.

computer code (GSF). The model is based on a generalized, reasonably fundamental description of the governing processes inside packed beds, including the ability to describe the solid-phase motion, and to handle the various time scales associated with several important phenomena (including ignition, changes in injection composition, tracer injection, and burnout of a bed). Because much past work has focused on models developed for specific issues by making simplifying assumptions, their general applicability is limited. On the other hand, a generalized model need not introduce simplifying assumptions to address a variety of questions, albeit at the possible expense of computational efficiency. Moreover, a single model can also serve as a test bed for developing simplifying assumptions to be employed by more comprehensive models.

A preliminary mathematical model was developed last year (Thorsness and Kang, 1984). Here we present further work, including model improvements and partial verification runs.

Specifically, we incorporated : better wall transport, axisymmetric geometry, more transient models, more reactions and species (8 reactions and 7 species), more options on boundary conditions, rezoning capability, injection of gas or heat anywhere in the bed, and temperature-dependent physical parameters. An LLNL report by Thorsness and Kang (1985) describes details of these developments.

#### FORMULATION

The following assumptions are introduced.

1. Temperature: Equal gas and solid temperatures at a given point in space;
2. Species: Two solid species (carbon and ash) and seven gas species (nitrogen, oxygen, hydrogen, carbon monoxide, carbon dioxide, water vapor, and methane);
3. Geometry: One or two-dimensional (including axisymmetric);
4. Gas Phase: Ideal gas law;
5. Gas phase: Darcy's law;
6. Solid phase: Three cases are analyzed :
  - (a) the solids are stationary ;
  - (b) the solid velocity is prescribed at a constant value in the vertical direction, and zero in the horizontal direction ;
  - (c) a simple bed-settling model, taking the overall-bed density to be constant and the solids moving straight downward.
7. Heterogeneous Reactions: For the solid particle-gas reactions, two kinetic model reactions are used. These are AS and SP models, the term AS denoting "ash segregation", and SP "shell progressive", respectively. More on this later.
8. Ash: Fixed ash particle size (at some fraction of the original particle size).
9. Wall region: In the wall region, a thin region exists through which thermal energy is exchanged such that a conventional heat transfer coefficient adequately characterizes the transport phenomena.

The above model is a compromise between completeness and expediency. We wanted to introduce sufficiently comprehensive model to permit evaluation of the usefulness of the current approach, yet not expend an undue amount of time developing detailed model physics. Additional features will be specified and discussed in the text as they occur.

#### Gas-phase mass-balance equation.

Overall gas conservation :

$$\frac{\partial(\phi C)}{\partial t} = -\nabla \cdot (\nabla \phi C) + \sum_{i=1}^n Q_i + \sum_{j=1}^n S_j \quad (1)$$

A definition of all variables is listed at the end of the paper in the Nomenclature section.

The effective gas velocity ( $v$ ) is related to the superficial and interstitial velocities as follows. The superficial velocity ( $U$ ) is a convenient term describing an average velocity with which the gas flows through the total cross-sectional area of the bed.

In our model we include porosity both internal and external to the solid particles. The superficial gas velocity is then the product of the total bed porosity and the effective gas velocity. The interstitial gas velocity signifies the velocity with which the gas flows through a local void area (Sherwood, et al. 1975), and is physically a more realistic property. In mathematical form we have:  
 $U = \phi_e v_{int} = \phi v.$

Conservation of Gas species:

$$\frac{\partial(\phi c_i)}{\partial t} = -\nabla \cdot (\bar{v} \phi c_i) + Q_i + s_i + \nabla \cdot (CD \nabla y_i) \quad (2)$$

Mass Balances (Solid-phase).

Overall solid conservation :

$$\frac{\partial[(1-\phi)\rho_s]}{\partial t} = -\nabla \cdot [(1-\phi)\rho_s \bar{v}_s] + \sum_{k=1}^{k=m} s_k' \quad (3)$$

Solid species conservation:

$$\frac{\partial[(1-\phi_e)\rho_s w_k]}{\partial t} = -\nabla \cdot [(1-\phi_e)\rho_s w_k \bar{v}_s] + s_k' \quad (4)$$

Although the overall equation is simply the sum of the individual species conservation equations, it is included here because we use these relationships to calculate the gas- and solid-phase velocities.

Conservation of Energy.

The energy balance for the entire system, in which we invoke the assumption of identical gas and solid temperature (Assumption 1), is given by:

$$\frac{\partial[\phi \sum_{i=1}^n (c_i h_i) + (1-\phi_e)\rho_s \sum_{k=1}^m (w_k h_k')] }{\partial t} = -\nabla \cdot [\sum_{i=1}^n (h_i \bar{j}_i)] - \nabla \cdot [\rho_s \bar{v}_s \sum_{k=1}^m (w_k h_k')] + W + \nabla \cdot (k \nabla T) \quad (5)$$

where the term  $j_i$  denotes total flux of gas species  $i$  and is given by  $j_i = \phi v c_i - CD \nabla y_i$ .

Equation of State.

In line with the ideal gas assumption, we have:

$$P = CRT \quad (6)$$

In Eqs.(1)-(6), there are  $10 + 1 + k$  dependent variables. Of these, the static enthalpy term  $h_i$  is a function of  $T$  and  $c_i$ , while the static enthalpy term for solid phase ( $h_k^*$ ) is a function of  $T$  and  $w_k$ . Also, the velocity terms  $U$  and  $v$  are related by  $v = U/\phi$ ,  $y_i$  and  $c_i$  are related by  $y_i = c_i/C$ , thus reducing the number of unknowns to seven. We therefore need an additional equation to completely define the flow characteristics. This is accomplished by relating  $v$  and  $P$  invoking Darcy's law (Assumption 5) --- see Eq. (7).

Once these dependent variables are calculated from solution of the partial differential equations, other parameter values, such as the porosity, can be determined from relevant relationships already derived (Thorsness and Kang 1984). We now give details of these steps.

Gas motions.

In the present formulation we do not explicitly use the overall mass balance equations for both the gas and solid phases; instead, we expand the equations to derive expressions for gas and solid velocities. In line with Assumption 5, we invoke Darcy's law in the gas phase, i.e., velocity and pressure in the bed are related by

$$\bar{U} = -(\Gamma/\mu)\nabla P \quad (7)$$

When this equation is substituted in Eq. (1), the gas velocities can be eliminated from the equation. After substitution and by using the ideal-gas law, the equation can either be viewed as an equation for pressure ( $P$ ), or for bed gas distribution ( $\phi C$ ). To maintain a conservative form we choose the latter and obtain the gas velocity through appropriate back substitutions.

Solid-phase motions.

For the flow physics of the solid phase, we conceptualize three situations (Assumption 6). The first is the absence of any solid motions, that is,  $v_s = 0$ . For this case, Eq.(3) for

the overall solid is not required and therefore is not used. In the second situation we envision a uniform solid flow in one direction, and we set the solid velocity at a constant value in the bulk flow direction and at zero in the horizontal direction, i.e.,

$$\begin{aligned} v_s &= \text{constant (y-direction), and} \\ v_s &= 0 \quad (\text{x-direction}). \end{aligned}$$

The third situation represents our first attempt at characterizing the solid-settling behavior in packed beds in a more general manner. Here we assume that the overall bed density remains constant and that the solids only move in a downward direction, i.e.,  $(1-\phi_s)\rho_s = \text{constant}$ . This removes the transient term from Eq. (3) and allows the equation to be integrated in the vertical direction, yielding the solid velocity as a function of position and time

$$v_s(y,t) = v_{s0} + \frac{1}{\rho_s} \int_{y=0}^y s'_c(y,t) dy \quad (8)$$

#### Heterogeneous reactions -- AS and SP Models (Assumption 7).

To solve the system of differential equations (1)-(5), we need to derive expressions for the production rates  $s_i$  and  $s_k^*$ . This requires formulation of a physical model to characterize the solid-gas interactions. Here we extend the models of Yoon et al. (1978). Two basic kinetic models for the heterogeneous reactions have been derived. The models assume that the apparent rate of an individual reaction may be controlled by: (i) gas-film diffusion external to the particle, (ii) diffusion through an ash layer, (iii) diffusion into the reacting particle, or (iv) intrinsic surface reaction rate. A single initial particle size (monodisperse) is being used here for both models, but treatment of a more general case of various initial-size distributions is possible.

In the Shell Progressive (SP) model, a core of unreacted solid is assumed to be surrounded by a shell of ash. For the gas phase reactants to reach the unreacted core, they must not only diffuse through the external gas film, but also through this ash layer. On

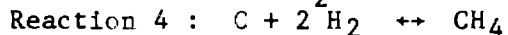
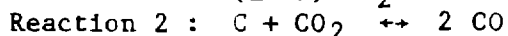
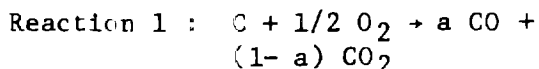
the other hand, the Ash Segregation (AS) model assumes that the ash falls away from the particle, leaving unreacted material exposed to the gas stream.

Because these two models should represent extremes in possible behavior, this fact enables us to bracket the magnitudes of the relevant reactions taking place in the bed. In both of these models the particle diameter plays a prominent role, it being a function of position in the bed and amount of reaction which has occurred. In the SP model the particle reaches a finite, minimum size during heterogeneous reactions (because of the ever-thickening ash layer surrounding the particle as the fraction of unreacted char goes to zero). This minimum size depends on initial particle size and ash concentration. By contrast, for the AS model the unreacted solid particle diameter can reach zero (because now there is no ash layer tending to inhibit reactions at the surface). The ash particle size is taken to be a certain fraction of the initial particle size (25% is used here -- see Assumption 8).

#### Reaction rates.

In characterizing the gas reacting with the solid in packed-beds, seven chemical reactions are used. Four are concerned with the heterogeneous reactions, i.e., carbon and other species. The fifth reaction, water-gas-shift (WGS), is quasi-heterogeneous in that the gas species are highly catalyzed by the presence of solid surfaces, such as happens in packed beds. The remaining three describe purely gas-phase reactions.

Heterogeneous reactions. There are four heterogeneous reactions for both AS and SP models. These are :



For the SP model the reaction rates are given in the form, adapted from Yoon, et al.(1978);

$$r_{SP} = \frac{\pi N (c - c_{eq})}{\frac{1}{k_c d_p^2} + \frac{1-F}{2D_e d_p} + \frac{6}{\eta k_r \rho_c d_u^3}} \quad (9)$$

Physically, the first term in the denominator in Eq.(9) signifies the bulk mass transfer of reactants to the particle surface, the second term the diffusion through the ash layer, and the third term the diffusion into and the intrinsic reactions at the surface of the unreacted core. The reactions are thus limited by these mechanisms.

With the AS model there is no ash layer and the reaction rate is given by

$$r_{AS} = \frac{\pi N (c - c_{eq})}{\frac{1}{1 - k_c d_p^2} + \frac{6}{\eta k_r \rho_c d_p^3}} \quad (10)$$

and is dependent on only two coupled mechanisms, i.e., bulk mass transfer of reactants to the particle surface, and diffusion and reaction in the unreacted particle.

#### Water-gas-shift reaction.

In addition to the above heterogeneous reactions we add the WGS reaction:



Even though it involves only gas-phase species, it is highly catalyzed by solid surfaces and as a result nearly all the reaction occurs on surfaces in a packed bed situation. For this reaction the same basic form as those given above are used, except that in the SP model the particles are taken to be uniformly active catalysts (i.e., no unreacted core is considered) and the rate is given by the AS model expression modified with appropriate particle diameters. On the other hand, the rates for AS model should account for the presence of both the unreacted particles and the ash particles. Therefore, we take the overall rate to be the sum of two rates, one using the

unreacted particle parameters in the AS expression and one using the ash particle parameters.

In both AS and SP models the intrinsic reaction rate of carbon and gas is expressed by the form

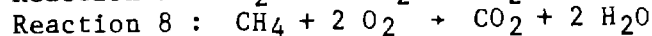
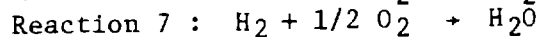
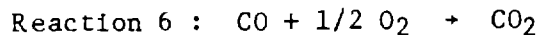
$$r' = A (c - c_{eq}) \exp(-E/RT) \quad (11)$$

The expression for the water-gas-shift reaction rate is taken from Govind and Shah (1984)

$$r_3 = 568RT \left(0.5 - \frac{P \times 10^{-7}}{2.53}\right) ([CO] - [CO]_{eq}) \exp(-13971/T) \quad (12)$$

The  $k_r$  used for this case in the overall rate expression includes everything except the carbon monoxide concentration.

Purely gas-phase reactions. We now consider three, strictly gas-phase reactions included here to allow gas-phase combustion. The reactions selected are



The rates for the reactions 6 through 8 can be expressed by the following form:

$$r_i = \frac{\phi_i c_2 A_i B_i Z_i \exp(-E_i/RT)}{1 + c_2 A_i B_i R_s \exp(-E_i/RT)} \quad (13)$$

wherein the term  $R_s$ , representing mass-transfer effects, was added to the reaction rate not so much for physical reasons but as a simple way of limiting gas-phase reaction rates at high temperatures. This will be discussed further in the section on the method of solution.

For CO combustion (reaction 6), we have, from Field et al.(1967):

$$A_6 = 4.75 (10^5); B_6 = 17.5 \\ c_6^{0.5} c_0^{0.3} / (C + 24.7 c_6); \\ Z_6 = c_4 R_{fact}(6); E_6 / R = 8050 \text{ K.}$$

For hydrogen combustion (reaction 7) is given by Peters (1979):

$$A_7 = 1.08 (10^{10}); B_7 = 1; \\ Z_7 = c_3 R_{\text{fact}}(7); E_7 / R = 15150 \text{ K.}$$

Finally, for methane combustion (reaction 8) is, from Sohrab et al. (1984):

$$A_8 = 4.33 (10^4); B_8 = 1; \\ Z_8 = c_7 R_{\text{fact}}(8); E_8 / R = 23,200 \text{ K.}$$

#### Transport properties.

In Eqs.(1)-(5), many transport and physical properties are involved. In particular, four physical properties, i.e., the absolute fluid viscosity, the specific heat of the gas, the heat capacity of the solid, and the thermal conductivity of the solid, are expressed in the model as a linear function of temperature. Also, the Prandtl and the Schmidt numbers are reasonably constant at 0.6 for the conditions of present interest. Therefore, the gas phase diffusivity and thermal conductivity can be obtained from known gas viscosity and specific heat, Prandtl number, and Schmidt number. An extension of property dependence on composition is straightforward but not included in the current model.

We also need expressions for the effective mass and thermal dispersion coefficients in both the axial and the radial directions because the gas species have to flow through the void spaces between the solid particles in packed-bed flows. Much work has been done on determination of these flow characteristics ( e.g., Coberly and Marshall 1951, Yagi and Kunii 1957, Bischoff and Levenspiel 1962, Edwards and Richardson 1968, Olbrich and Potter 1972, Schlunder 1978, Dixon and Cresswell 1979, and Wakao and Kaguei 1982). We choose the following:

$$\begin{aligned} &\text{o Effective Mass Dispersion -} \\ &\text{Perpendicular (Bischoff 1969);} \\ &D_p^{\text{eff}}/D_g = 0.73 + 0.1 \text{ Re Sc} \end{aligned} \quad (14)$$

$$\begin{aligned} &\text{o Effective Mass Dispersion - Flow} \\ &\text{(Edwards and Richardson 1968);} \\ &D_f^{\text{eff}}/D_g = 0.73 + 0.5 (\text{Re Sc})^2 / \\ &\quad (9.7 + \text{Re Sc}) \end{aligned} \quad (15)$$

$$\begin{aligned} &\text{o Effective Thermal Transport -} \\ &\text{Perpendicular (Wakao and Kaguei 1982);} \\ &k_p^{\text{eff}}/k_g = k^0/k_g + 0.1 \text{ Re Pr} \end{aligned} \quad (16)$$

$$\begin{aligned} &\text{o Effective Thermal Transport - Flow} \\ &\text{(Wakao and Kaguei 1982).} \\ &k_f^{\text{eff}}/k_g = k^0/k_g + 0.5 \text{ Re Pr} \end{aligned} \quad (17)$$

Here the subscript f refers to the local flow direction and p the direction perpendicular to the flow. In the model we assume that these components can be mapped onto the required x and y directions by constructing an elliptical variation of magnitudes between f and p components. At high temperatures the effective thermal conductivity becomes much greater than the physical thermal conductivity, principally because of the radiative effects becoming dominant at high temperatures, typically above 1300 K. Details are given in Thorsness and Kang (1985).

#### Boundary conditions.

For solids, we consider three situations, consistent with Assumption 6. These are: stationary solids, constant solid velocity, and the solid velocity determined from Eq.(8), based on the constant-bed assumption. Thus we prescribe either the flux or the velocity of the solids being removed at the bottom plane counter to the gas flow direction, see Eq.(8).

For other dependent variables (such as the species and the temperature), the boundary conditions are more complicated, and we list them at four boundaries encompassing the packed-bed flow field, i.e., the inlet plane, the exit plane, the centerline axis, and the wall region (see Figure 1 ).

(a). Inlet Plane . For species, we prescribe flux values, i.e.,  $f_1 = j_1$ . For thermal balances, we impose the condition:

$$\left( \sum_{i=1}^n f_i h_i \right)_{y=0^-} = \left( \sum_{i=1}^n j_i h_i \right)_{y=0^+} - (k \partial T / \partial y)_{y=0^+} \quad (18)$$

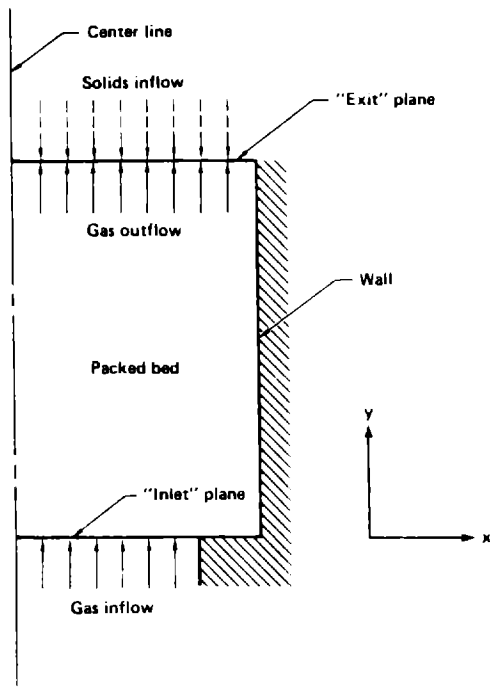


Figure 1. Packed Bed Geometry (Schematic).

In this equation, the injection temperature and flow are known (prescribed at  $y=0^-$ ), while the temperature and its gradient at the inlet position (at  $y=0^+$ ) are to be obtained as part of the solution. For cases where the temperature gradient is zero at the inlet plane, the equation degenerates to specifying the inlet temperature equal to the temperature at the bed bottom. If solids leave the bottom, we assume that they leave at temperature  $T(x,0)$ .

(b). Exit Plane. For species at the outflow plane, we impose the zero-gradient condition, i.e.,  $dc_i/dy = 0$ . For the energy-balance, we have a radiant heat-exchange capability with the surroundings. Thus we have :

$$-k \partial T / \partial y = S (T^4 - T_\infty^4) \quad (19)$$

For zero radiation this simplifies to a zero-gradient condition.

(c). Centerline. For all dependent variables (species and temperature), we impose axisymmetric condition, i.e.,  $dF/dx = 0$ , where  $F$  is any dependent variable.

(d). Wall Region. The wall region is defined to be both the vertical wall and the portion of the bottom plane which has no inlet flow. To accommodate various thermal and chemical interactions at the wall boundary, we introduce many optional boundary conditions, including wall-regression due to char formation.

For species, we introduce two possible situations :

(i). No flux at the wall:  $dy_i/dz = 0$ . Here  $z$  is the appropriate dimension perpendicular to the wall.

(ii). Finite species flux related to the heat-transfer characteristics and the wall drying/pyrolysis model.

For thermal energy balances in the wall region, we have :

(i). Adiabatic wall:  $dT/dz = 0$ .

(ii). Heat exchange with the flow through heat-transfer coefficient

a. Isothermal wall temperature, i.e., infinitely large heat-transfer coefficient.

b. Variable wall temperature, with either prescribed magnitude for the heat-transfer coefficient, or a built-in correlation for heat transfer between the flowing medium and the wall region. This condition can also accommodate the wall-regression case, for which case appropriate relationships can be specified independently for the side and the bottom walls with some restrictions.

#### METHOD OF SOLUTION

The partial differential equations (PDE's) described above are solved by using a method-of-lines (MOL) approach. This scheme was chosen because (1) it is flexible in formulating the physics of a given problem, (2) changes are easily implemented, and (3) it can naturally handle 1, 2 or even 3 spatial dimensions as well as the various time scales. Moreover, the method has been successfully applied to the related problem of oil shale retorting by Hindmarsh (1983).

The MOL scheme is based on the solution of a set of initial-value ordinary differential equations (ODE's). These ODE's are obtained from the PDE boundary value problem of interest by discretizing the PDE's in the spatial dimensions. This yields a set of ODE's with time as the independent variable. A suitable ODE solver is then used to integrate the system of equations in time, to yield the required solutions. The power of the method stems primarily from choosing one of the very powerful ODE solvers currently available. The ODE solver must be able to handle the stiff system which results from the discretization of the spatial dimensions and physics of the problem. It should also provide a straightforward method of time step and error control. The ODE solver used here is LSODE, a widely available software package developed at LLNL by Hindmarsh (1980). LSODE provides the user with a number of options in solving a system of ODE's. We select option mf=25, which uses an internally generated banded Jacobian to solve a stiff equation set. The bandwidth is related to the number of dependent variables as well as the number of cells in the x (Cartesian or radial) direction.

The use of the Jacobian represents both the power and the limitation of the solution scheme. The Jacobian is a matrix defining the partial derivative of dependent variables with respect to other dependent variables, and represents a method by which the equations are linearized, a key step in the solution of the ODE's. However, the size of the Jacobian can get quite large. Thus the major computer limitation arises in dealing with the storage of this Jacobian. The number of floating point values (fp's) required by LSODE for this and other purposes is given approximately for our problem by the formula

$$\text{fp's} = 10 n_{eq} + 3 (n_x + 2) (n_y - 1) n_{eq}$$

where  $n_{eq}$  is the number of equations,  $n_y$  is the number of dependent variables in the problem, and  $n_x$  is the number of cells in the

x-direction. The number of equations,  $n_{eq}$ , to be solved by LSODE is given by  $n_{eq} = n_x \cdot n_y \cdot n_v$  where  $n_y$  is the number of cells in the y-direction. For a one dimensional problem this size constraint is not serious. For a problem in which seven gas species are used a 360 cell problem can be contained entirely in the memory of a 400k word CDC 7600 and a 1800 cell problem in a 2 million word CRAY. Size constraints however are much more limiting for a two dimensional problems. For a 7 gas species problem only a 11x8 ( $n_x \cdot n_y$ ) problem can fit on the CDC 7600 and a 41x11 problem on a CRAY. If, however, only three gas species are used in a two-dimensional problem then an 11x21 problem will fit on the CDC 7600 and a 11x101 problem on the CRAY.

Unlike the computer memory requirements, general statements cannot be made on computation time requirements, because the computation time depends not only on the problem size but the problem physics. As an example, a 1 mol/s-m<sup>2</sup> flow of 2:1 steam:oxygen mixture would gasify 1/3 of a one-dimensional char bed 1 meter long in 8 hours. The computation times on CDC 7600 time for this gasification process using seven species were 363 s for 11 nodes, 1105 s for 21 nodes, and 2845 s for 41 nodes. These times are larger than previously reported in Thorsness and Kang (1984). Analysis reveals that only a small increase in computation time was due to variable properties; rather, the more stringent error control currently being applied in LSODE seems to be causing increased computation times. A further feel for computation time is provided in the following discussion of the validation and example runs.

In developing the discretized equations fairly standard finite difference methods were used. Wherever possible the conservative form of the equations was preserved. Also upwind or donor cell differencing of the convective terms was used to protect against the formation of spatial wiggles in convected quantities. Spatial wiggles

cannot be tolerated since they can lead to nontrivial negative concentrations which are difficult to handle. The price for removing the wiggles in this fashion is an increase in numerical dispersion, which can only be reduced by using finer cells. Details are given in Thorsness and Kang (1985).

The resultant computer code (called GSF code) is quite flexible in that various boundary conditions, initial conditions, geometry and problem physics can be specified through the input data. This includes the ability to select from a list of seven gas species built into the code. For problems requiring only a few gas species the ability to solve the equations leads to a large savings in computer resources. The code is modular enough that additional gas species and new kinetic or transport correlations can easily be added. This however does require a recompilation. The code is designed so that a given problem can be repeatedly restarted from any desired point in its evolution and new problem parameters can be specified. This can greatly reduce the computational effort in doing parameter studies as well as provide a means of recovering from minor computing problems that may arise. Finally, to maximize flexibility of output two post-processor codes are used to tabulate or plot selected data from computed results. These codes can be run repeatedly to display different aspects of a single computational run.

As a result of the robust nature of the solution scheme, few compromises had to be made in the physical description of the problem to facilitate the numerical solution. Two features, however, have been added: (1) In the reaction rate routine, special coding is instituted so that two small negative concentrations do not result in a positive rate; (2) An artificial mass transfer resistance in the gas phase oxidation rate expressions. This is modeled after the gas-film resistance of the heterogeneous reactions and is a simple way of limiting the oxidation reaction rate at high temperatures. This resistance is

controlled through an input parameter so that it offers no resistance, is equal to that for the heterogeneous reactions, or any fraction of the gas-film resistance of the heterogeneous reactions. This allows the gas-phase oxidation to be finite yet prescribed so that it is everywhere some multiple times larger than any of the heterogeneous rates. We usually set the parameter to 0.2, limiting the gas-phase oxidation rates at least five times larger than any of the heterogeneous reactions. As a final practical matter we have found that on occasion the calculation will sometimes yield a branch solution with negative concentrations. Our code can detect this, and restarting the problem at a point just prior to the problem area provides a successful solution.

#### VERIFICATION RUNS

To validate the models and the numerical approach embodied in the GSF computer code, we have performed calculations involving steady and transient flows, moving thermal and concentration waves, gasification, 1-d and 2-d, and wall heat transfer. Comparisons of the GSF computer results and the appropriate analytic solutions demonstrate good agreements; for brevity only certain cases are treated here, with other details being given in Thorsness and Kang (1985).

For these validation runs we use the following reference physical conditions: Viscosity =  $5.4 \text{ E-}05 \text{ kg/m-s}$ ; Permeability =  $1.0 \text{ E-}11 \text{ m}^2$ ; Exit pressure =  $1.0 \text{ E+}05 \text{ Pa}$ ; Temperature (initial) =  $300 \text{ K}$ ; Flow rate (gas) =  $1 \text{ mol/m}^2\text{-s}$ ; Tube length =  $1 \text{ m}$ ; Tube width (or radius)  $1 \text{ m}$ ; Original gas in tube = Nitrogen (inert); Effective mass dispersion =  $5.0\text{E-}4 \text{ m}^2/\text{s}$ ; Effective thermal conductivity =  $1.2 \text{ W/m-K}$ . Unless otherwise noted, these values were used for all cases.

#### Motion of a Transient, One-dimensional Concentration Wave.

When a gas is injected into a packed bed filled with an inert gas different from the injected gas, diffusion as

well as convection of the injected gas takes place as it flows through the packed bed. The case considered here is: one dimensional, no reactions, no solid motion, isothermal, (oxygen) injected gas, (nitrogen) original gas in bed, axial dispersion, and constant porosity.

Under these conditions the only nontrivial equation is the species equation (2), which reduces to :

$$\frac{\partial c_i}{\partial t} + v \frac{\partial c_i}{\partial y} = D \frac{\partial^2 c_i}{\partial y^2} \quad (20)$$

with the boundary conditions

$$t = 0 ; \quad c_i = c_{i0}$$

$$y = 0 ; \quad v c_i - D \partial c_i / \partial y = v c_{in}$$

$$y = L ; \quad \partial c_i / \partial y = 0$$

The differential equation (20) has been solved analytically by Brenner (1962). We shall use his asymptotic solution for comparison with our GSF code calculation results. The specific conditions used are :  $C = 12 \text{ mol/m}^3$ ,  $D = 5.0\text{E-}4 \text{ m}^2/\text{s}$ ,  $v = 0.8 \text{ m/s}$ . Figure 2 shows the analytic solution as well as the GSF results with 26 and 201 nodes at  $t = 15$  seconds. For the latter case only selected points are plotted in the figure for clearer comparison. The case of 25 nodes is reasonably close to the analytical solution, but much better agreement is noted between

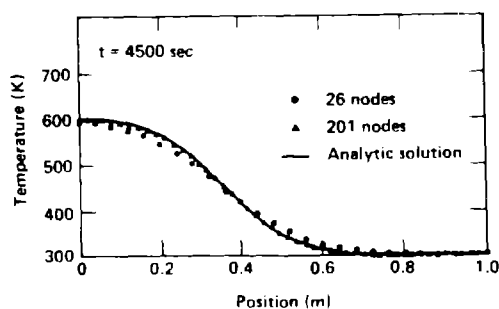


Figure 2. Comparison between Analytic Solution and GSF Calculations for a One-dimensional Concentration Wave Inside a Packed Bed ( $t=15 \text{ sec.}$ ).

the analytical solution and the 201-node case. The CPU times on a CDC-7600 for these waves to encompass the entire bed ( $L=1 \text{ m}$ ) were 14 s for 26 nodes, 28 s for 51 nodes, 63 s for 101 nodes, and 176 s for 201 nodes. This indicates that increasing the number of nodes increases the CPU by a factor slightly greater than the node multiplication factor.

The case of a moving thermal wave also gives very good agreement between the GSF code results and the analytical solution also obtainable from Brenner (1962). Although the thermal wave and the concentration wave are similar, physically these two wave motions possess widely differing time scales of motion. Whereas the oxygen wave moves through the bed in less than a minute, the thermal wave moves much more slowly, consuming more than two hours to encompass the length of the bed ( $L=1 \text{ m}$ ). This is due to the large heat capacity of the solid particles inside the packed bed. the CPU times for the GSF runs on 7600 computer were 19 s for 26 nodes, 42 s for 51 nodes, 107 s for 101 nodes, and 202 s for 201 nodes. We thus conclude that the GSF code can calculate and produce similar solutions (e.g., thermal and concentration waves), by integrating different PDE's with widely variant propagation velocities.

#### Catalyst Regeneration Problem.

This problem is often encountered in designing reactors for cracking or dehydrogenating hydrocarbons, where regeneration is employed to remove coke deposits from the catalyst bed. Removal is effected by oxidation, which generates a high temperature peak in the reaction zone where burning of the coke is taking place. This reaction zone then travels down the bed, purging coke in its path. Such a case is studied here, i.e., the regeneration of a catalyst bed by oxidation of contaminants. The problem is idealized to the case of introducing oxygen and nitrogen at the inlet of a packed bed containing inert particles with a small fraction of carbon. The bed is initially at temperature  $T_0$ . Only

carbon combustion is allowed, i.e.,  $C + O_2 \rightarrow CO_2$ . For analytic case the specific conditions used are : one dimensional, constant flow rate, constant properties, no solid motion, no mass dispersion, no thermal dispersion, two gas species (oxygen and nitrogen), carbon combustion only, and zero-order reaction (independent of temperature).

Under these conditions Eq.(2) becomes :

$$\frac{\partial(\phi c_{O_2})}{\partial t} = - \frac{\partial(U c_{O_2})}{\partial y} + s_{O_2} \quad (21)$$

Eq.(4) becomes :

$$\frac{\partial[(1-\phi_c)\rho_s w]}{\partial t} = s^* \quad (22)$$

Eq.(6) becomes :

$$[\phi \rho_g c_g + (1-\phi_c)\rho_s c_s] \frac{\partial T}{\partial t} = - \frac{\partial(U \rho_g c_g T)}{\partial y} + \rho_s L^* B \quad (23)$$

where  $L^*$  denotes the heat of reaction and  $B$  the production (or loss) rate of carbon. Since  $c_{O_2}$  (oxygen) and  $w$  (solid carbon) react with each other in combustion,  $s_{O_2}$  and  $s^*$  are related to each other and to  $B$ .

Analytic solutions to Eqs.(21)-(23) have been obtained by Johnson, et al. (1961) and by Thorsness, et al. (1978). Details are given in Thorsness and Kang (1985). Using the GSF code, sample calculations were performed for initial bed temperature of 600 K, giving a reaction wave which proceeds downstream as a function of time. Results are given in Figures 3 and 4 at  $t = 427$  sec with 101 nodes for the GSF code calculations. Figure 3 shows the carbon and the oxygen distributions along the bed. Also shown is the analytic solution, which compare favorably with the GSF results. The temperature distribution is given in Figure 4. The profiles agree well with each other except in the reaction region, where the analytic result is more peaked than the GSF result. This discrepancy can be attributed mainly to the fact that the upwind difference used for stability in GSF code unavoidably introduces some

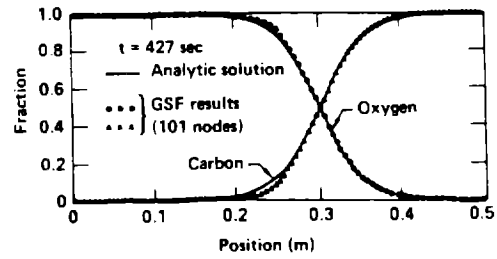


Figure 3. Comparison between Analytic Solution and GSF Calculations for a Gas and Solid Distributions for a One-dimensional Catalytic Regeneration Flow ( $t=427$  sec.)

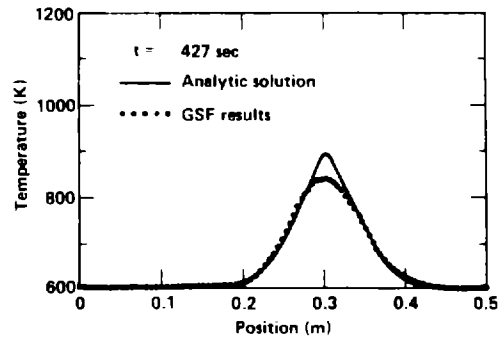


Figure 4. Comparison between Analytic Solution and GSF Calculations for Temperature Distribution in the Reaction Zone of a One-dimensional, Catalytic Regeneration Flow ( $t=427$  sec.).

dispersion into the problem. This dispersion can only be made identically zero by using an infinite number of nodes. In real systems some dispersion is always present; however, the analytic solution is only exact for zero dispersion. Therefore, the agreement is deemed acceptable.

#### Steady, Two-dimensional Flow with Wall Heat Transfer.

This type of flow is often employed to measure the effective thermal conductivities in packed-bed flow situations (e.g., Wakao and Kaguei 1982). Consider a cylindrical packed bed operated as a heat exchanger, that is, steady state, uniform flow, no reactions, no new gas introduced, no solid motion, constant wall temperature, one gas species (nitrogen), and constant physical properties.

Under these conditions only Eq.(5) is nontrivial, and it reduces to :

$$G c_p \frac{\partial T}{\partial y} = \frac{1}{x} \frac{\partial (x k_x \frac{\partial T}{\partial x})}{\partial x} + k_y \frac{\partial^2 T}{\partial y^2} \quad (24)$$

with the boundary conditions

$x = 0$  (centerline) :

$$\frac{\partial T}{\partial x} = 0 \quad (\text{symmetry condition})$$

$x = R$  (wall) :  $-k_x \frac{\partial T}{\partial x} = h(T - T_w)$ ;

$y = 0$  (inlet) :  $T = T_0$  .

The last condition states that the inlet temperature is maintained at a prescribed value  $T_0$ . (Usually the inlet temperature is different from the injected temperature by the thermal gradient existing at the inlet.)

Analytic solution to Eq.(24) with these boundary conditions is given by Wakao and Kaguei (1982). Also, calculations were made on the GSF code for a bed (0.5 m long) initially at 900 K. At time  $t = 0$ , the inlet temperature is raised to, and maintained at, 1000 K. The results are shown in Figure 5, which shows a slow decrease in the centerline temperature along the bed, while the near-wall temperature shows a steep decrease immediately after the inlet region, reflecting strong heat-transfer activity there. When we compare the results from the GSF code (with  $6 \times 21$  nodes) with the analytic

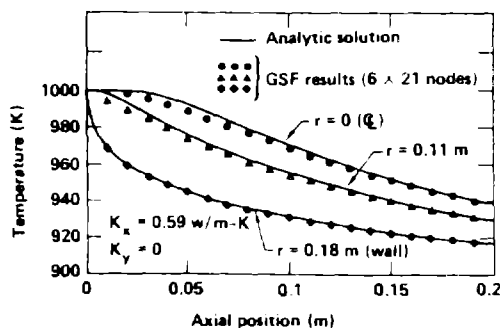


Figure 5. Comparison between Analytic Solution and GSF Calculations for Temperature Distribution in a Non-isotropic Bed for Two-dimensional Flow with Wall Heat Transfer.

solutions, we obtain good agreement everywhere except near the inlet region. This discrepancy is due to the use of a simpler analytic solution, which assumes identical injected gas and bed-bottom temperatures. Despite this, the two results are close enough to confirm that the present GSF code can calculate accurately the two-dimensional heat transfer situations in a packed bed.

#### SAMPLE PROBLEMS RELATED TO UCG PHENOMENA

We now apply the GSF code to several UCG-related situations : wall drying; and wall regression during gasification. (Water injection into a gasifying bed has also been calculated; details are given in Thorsness and Kang - 1985. )

##### Wall Drying.

Understanding the physics of growth of a rubble-filled gasification cavity is important in determining the ultimate cavity width dimension and the resource recovery in in-situ coal gasification. Grens and Thorsness (1984) have suggested that the growth is directly linked to the rate of heat transfer from a hot rubble bed to a drying/pyrolyzing coal wall. To explore the fundamental aspects of this mechanism a series of experiments is being undertaken by Grens at U.C. Berkeley. The first in this series of experiments will look at the simple model system of a uniform non-reacting bed with hot gas flowing through it and a water saturated wall. The rate of drying of the wall and thus the rate of heat transfer to the wall will be examined in a cylindrical vessel with the hot gas flow entering at the bottom center.

The GSF code has been used to perform some preliminary modeling of a related system for a cylindrical reactor of radius 5 cm and height 25 cm filled with a low density spherical packing 1.25 cm in diameter creating a uniformly permeable bed. The walls are assumed to be kept saturated with water and are evaporating into the hot gas flow. Gas flux (nitrogen) of 8 mmol/s

(1 mol/s·m<sup>2</sup> of bed) are injected at 900 K while the initial bed temperature is 300 K. The wall model described in Thorsness and Kang (1985) is applied at the evaporating walls. The bottom of the bed is assumed to operate adiabatically. Preliminary runs yielded virtually identical results for one gas and for two gases (N<sup>2</sup> and H<sub>2</sub>O), demonstrating the adequacy of runs with only one gas in the system. Many runs were made using a variety of cell numbers. The results show that the average drying rate can be fairly estimated even with a very coarse 3x3 system.

Figures 6-9 present selected results obtained using a 6x11 system. In Figure 6 the time to reach steady-state is compared for a range of injected gas flow rates. The time to reach steady-state increased rapidly with decreasing flow rate, ranging from about 100 seconds for the 10 mol/s·m<sup>2</sup> case to 5,000 seconds (2.8 hrs) for the 0.1 mol/s·m<sup>2</sup> case.

Figure 7 shows the average wall drying rate as a function of injected gas flow. The slope of the flow rate vs. drying rate on the log-log plot ranges from about 1 at the low flow to about 0.8 at the high flow. The 0.8 power dependence at the high end is clearly consistent with the heat transfer correlation 0.8 dependence. On the low flow end the unity power dependence is not a result of the heat transfer flow dependence (which is 0.5), but rather reflects the fact that the limiting

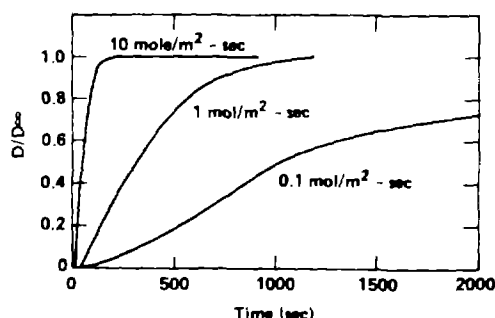


Figure 6. Drying-rate History for Three Flow Rates (Wall-Drying Problem ).

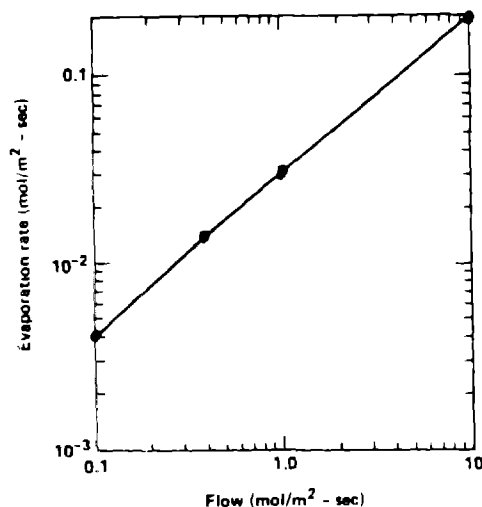


Figure 7. Drying Rate vs. Flow Rate (Wall-Drying Problem ).

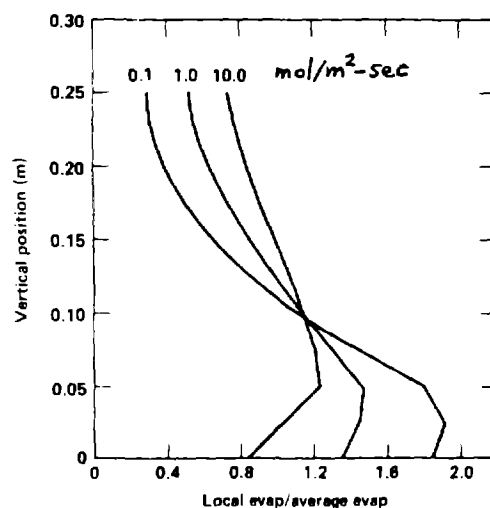


Figure 8. Distribution of Drying Rates along Bed for Three Flow Rates (Wall-Drying Problem ).

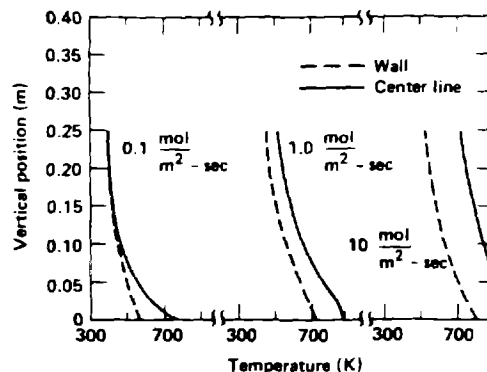


Figure 9. Temperature Profiles at Wall and Centerline for Three Flow Rates (Wall-Drying Problem ).

factor is the total heat injected. That is, at the very low flows the exit gas leaves the bed at the steam temperature and thus the drying rate is limited by the available energy in the injected hot gas.

In Figure 8 the local evaporation rate vs. vertical position in the bed is shown at steady state for three flow rates. The rate is more uniform for the high flow case ( $10 \text{ mol/m}^2\text{-s}$ ) where the energy input is not limiting. Finally in Figure 9 the calculated wall and center-line temperatures are plotted for the three flow rates. The heat limitation is clearly shown here by the coincidence of the wall and center line temperatures near the top of the bed for the low flow case.

#### Wall Regression during Gasification.

The problem of interest here is related to small cavities and to our proposed simulated coal seam experiments. These experiments would utilize a synthetic coal seam approximately 5 ft (1.5 m) thick. The model system on which calculations were performed is 1 meter in radius and 1 m high, filled with rubble material consisting of ash in the center and char near the walls and at the top. The walls are coal which can pyrolyze and produce gas and char. A 2:1 steam:oxygen mixture is injected at a rate of 6 mol/s into the bottom center of the bed. A series of computer runs were made to determine what thickness of char bed at the wall would lead to a self sustaining system. By self sustaining simply means that calculated char bed production at the wall, estimated via the wall model of Thorsness and Kang (1985), is equal to the rate of char being consumed near the wall (but inside the bed).

Calculations were performed using all seven gas species on a 6 x 6 grid. The initial bed temperature was set at 900 K so that the bed would reach a fairly steady thermal profile before too much of the bed carbon was consumed. A fairly steady state was reached after about one hour of real time. To compute the complete transient during start-up leading to this steady-state required

35-40 minutes of computer time on a CDC 7600 machine.

Figure 10 shows the rate of carbon production computed at the walls and the amount of carbon consumed in the bed as a function of three different char layer thicknesses. The computed wall regression rate, and thus the computed carbon production rate, was very nearly constant in all three cases, while the carbon consumption varied more or less linearly with char thickness. The linear variation of carbon consumption is clearly related to the greater abundance of carbon in the bed and the decrease in distance between the injection point and the char/ash transition. The wall regression rate indicates that the dominant resistance for heat transport to the coal wall is the wall layer heat transport and not the proximity of the char/ash transition. The figure also shows that the case with a 7.5 cm wall char thickness is close to a self sustaining system, at least on the average, since the rates of carbon consumption and carbon production are very nearly equal.

The bed temperature isotherms and gas flux near steady-state are shown in Figures 11 and 12 for the 7.5 cm char thickness run. The gas injection temperature is 400 K and the computed average wall temperature is 1100 K, while the exit gas temperature is 1700 K. The temperature gradient near the wall is not well represented by the coarse isotherms of Figure 11. The sharp gradient at the bed top is a result of the char layer present there. Although the average carbon consumption and production are nearly balanced for the 7.5 cm case, local rates show some variation. In particular, the carbon loss from the bed exceeds the carbon production at the wall in the bottom portion of the bed. This local disparity is shown in Figure 13. The rates over the top portion of the bed are, however, very nearly equal. This behavior would tend to develop a thinner char layer near the bed bottom.

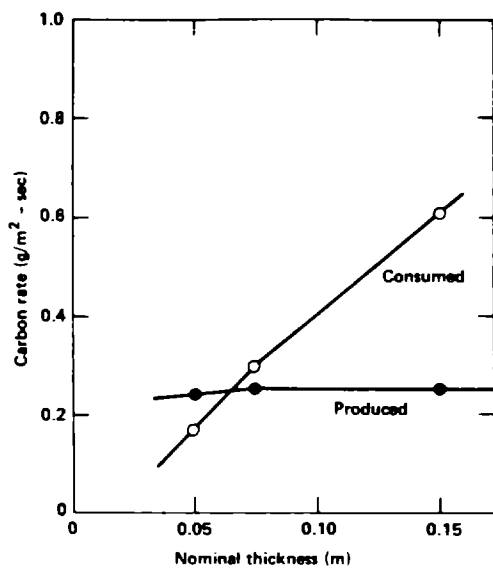


Figure 10. Carbon Production Rate vs. Wall Char-layer Thickness (Wall-Regression Problem ).

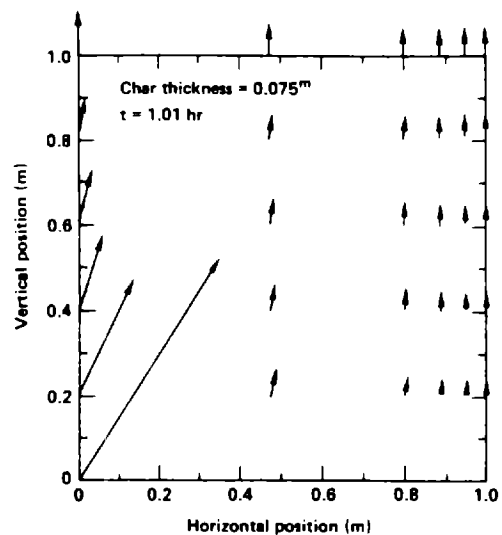


Figure 12. Local Gas-flux Distribution inside a Bed at  $t = 1.01$  hr (Wall-Regression Problem ).

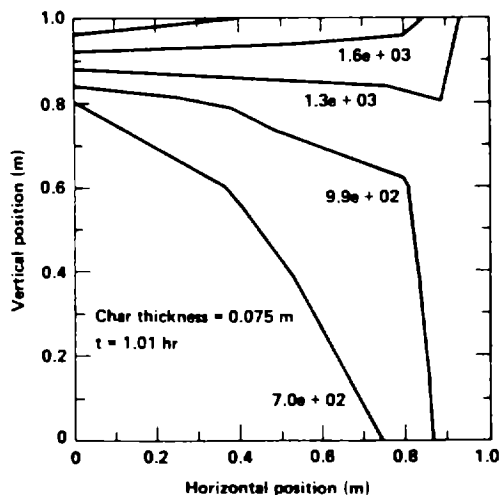


Figure 11. Temperature Distribution inside a Packed Bed at  $t = 1.01$  hr (Wall-Regression Problem ).

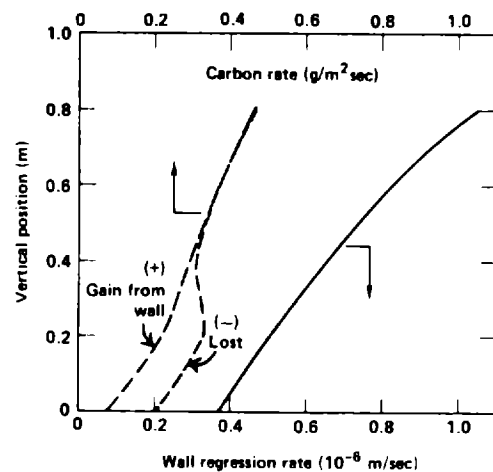


Figure 13. Local Carbon and Wall-regression Rates along Vertical Position in the Bed.

Also shown in Figure 13 is the computed local wall regression rates. They show that the bed wall would move outward more rapidly at the top than at the bottom in a truly self sustaining system. The average wall regression rate of  $7.7 \times 10^{-7}$  m/s is only 0.07 m/day. Thus, to obtain rates more characteristic of field results ( i.e.,  $\sim 0.5$  m/day) some additional physics not currently present in GSF computer code must be involved. The most likely candidate would seem to be a non-uniform permeability distribution. This hypothesis is explored in a recent related modeling work of Grens and Thorsness (1985).

place inside a synthetic coal (scale model); scoping of important mechanisms for packed-bed flows at various conditions of temperature, pressure, particle size, etc.; evaluating the validity of other simplified models; and modifying the present upwind differencing capability to improve the numerical intergration scheme. We also plan to continue analysis of the peak-temperature near the reaction front, the two-dimensional drying problem, the wall-growth problem, incorporation of the momentum equation into the model rather than using the Darcy equation, and the water-influx problem involved in the underground coal gasification phenomena.

## CLOSURE

A generalized model for describing reacting flows through packed beds has been presented. The model deals with transient flows, wall transport, many reactions and species (including methane), various options on the boundary conditions, rezoning capability, and variable transport properties, such as effective thermal and mass dispersions.

Results obtained from the present model (and the GSF computer code developed therefrom) show wide applicability of the code for characterizing various reacting flows through packed beds by yielding reasonable CPU times and by favorable agreements with other available studies for a variety of situations (such as concentration and thermal waves travelling at very different velocities, transient reacting wave motions, wall heat transfer, and wall regression).

The model has also been applied to the cases of wall drying, of a fluid injection, and of wall regression due to surface reactions. Some promising preliminary results are obtained; however, more analysis is needed before a definitive statement can be made on the applicability of the present model to these cases. Future plans include: use of the GSF code for detailed examination of the phenomena taking

# NOMENCLATURE

A	= Pre-exponential rate constant	(1/s)
B	= Reaction rate used in regeneration problem	(1/s)
C	= Total gas concentration	(mol/m <sup>3</sup> )
c <sub>i</sub>	= Concentration of gas species i	(mol/m <sup>3</sup> )
c <sub>eq</sub>	= Equilibrium concentration of a gas	(mol/m <sup>3</sup> )
c <sub>g</sub>	= Average gas heat capacity	(J/mol-K)
c <sub>s</sub>	= Average solid heat capacity	(J/kg-K)
d	= Diameter	(m)
d <sub>a</sub>	= Ash particle diameter	(m)
d <sub>p</sub>	= Particle diameter	(m)
d <sub>u</sub>	= Unreacted particle diameter	(m)
d <sub>0</sub>	= Initial particle diameter	(m)
D	= Effective superficial mass dispersion in bed	(m <sup>2</sup> /s)
D <sub>e</sub>	= Effective gas diffusivity inside a particle	(m <sup>2</sup> /s)
D <sub>m</sub>	= Average molecular diffusivity (m <sup>2</sup> /s)	
E	= Activation energy for rate constant	(J/mol)
F	= Fraction of original carbon remaining	
f	= Ash particle size fraction	
G	= Average molar gas flux	(mol/m <sup>2</sup> -s)
h	= Heat transfer coefficient	(W/m <sup>2</sup> -K)
h <sub>i</sub>	= Enthalpy of gas species i	(J/mol)
h <sub>k</sub> <sup>*</sup>	= Enthalpy of solid species k	(J/kg)
j <sub>i</sub>	= Total flux of gas species i	(mol/m <sup>2</sup> -s)
k	= Effective bed thermal conductivity	(W/m-K)
k <sub>c</sub>	= Gas film mass transfer coefficient	(m <sup>2</sup> /s)
k <sub>r</sub> <sup>*</sup>	= Reaction rate constant	(1/s)
L	= Heat of reaction	(J/kg)
M <sub>i</sub>	= Molecular weight of species i	(Kg/mol <sub>i</sub> )
m	= Number of solid species	
N	= Number of particles per volume of bed	(1/m <sup>3</sup> )
N <sub>a</sub>	= Number of ash particles per volume of bed	(1/m <sup>3</sup> )
n	= Number of gas species	
n <sub>v</sub>	= Number of dependent variables	
n <sub>x</sub>	= Number of nodes in x-direction	
n <sub>y</sub>	= Number of nodes in y-direction	
P	= Pressure	(Pa)
Q <sub>i</sub>	= Rate of species introduced into flow	(mol/m <sup>3</sup> -s)
r <sup>*</sup>	= Reaction rate per volume of bed	(mol/m <sup>3</sup> -s)
r <sup>*</sup>	= Intrinsic reaction rate	(mol/m <sup>3</sup> -s)
r <sub>1</sub>	= Intrinsic rate of reaction 1	(mol/m <sup>3</sup> -s)
R	= Gas constant	(J/mol-K) or (Pa-m <sup>3</sup> /mol-K)
s <sub>i</sub> <sup>*</sup>	= Species i gas source per volume of bed	(mol/m <sup>3</sup> -s)
s <sub>k</sub> <sup>*</sup>	= Solid species k source per volume of bed	(kg/m <sup>3</sup> -s)
s <sub>c</sub>	= Solid carbon source per volume of bed	(kg/m <sup>3</sup> -s)
Sc	= Schmidt number	
t	= Time	(s)
T(x,y,t)	= Temperature at position x,y at time t	(K)
T <sub>inj</sub>	= Injected gas temperature	(K)
T <sub>s inj</sub>	= Temperature of input solid	(K)
U	= Superficial gas velocity	(m/s)
v <sub>int</sub>	= Interstitial velocity	(m/s)
v	= Effective gas velocity	(m/s)
v <sub>s</sub>	= Superficial solid velocity	(m/s)
v <sub>s0</sub>	= Superficial solid velocity at the bottom of the bed	(m/s)

W	= Heat source introduced into the flow	(W/m <sup>2</sup> )
w <sub>a0</sub>	= Initial weight fraction of ash in solid	
w <sub>c</sub>	= Mass fraction carbon in solid	
w <sub>c0</sub>	= Initial weight fraction of carbon in solid	
w <sub>k</sub>	= Mass fraction of solid species k	
x	= Horizontal coordinate	(m)
y	= Vertical coordinate	(m)
y <sub>i</sub>	= Mole fraction of species i	
α	= Fraction of combusted carbon going directly to carbon monoxide	
ρ	= Gas density	(kg/m <sup>3</sup> )
ρ <sub>s</sub>	= Average density of solid particle	(kg/m <sup>3</sup> )
ρ <sub>c</sub>	= Carbon density in unreacted solid	(kg/m <sup>3</sup> )
ρ*	= Reactive solid density	(kg/m <sup>3</sup> )
φ	= Total porosity in the bed	
φ <sub>e</sub>	= Bed porosity external to particles	
φ <sub>int</sub>	= Porosity internal to a particle	
η	= Reaction effectiveness factor	
γ	= Permeability	(m <sup>2</sup> )
μ	= Average gas viscosity	(Pa-s)
τ	= Thiele modulus	

#### Subscripts

i = gas species:	1 - N <sub>2</sub> ;
	2 - O <sub>2</sub> ;
	3 - H <sub>2</sub> ;
	4 - CO ;
	5 - CO <sub>2</sub> ;
	6 - H <sub>2</sub> O ;
	7 - CH <sub>4</sub>
k = solid species:	1 - carbon ;
	2 - ash

#### ACKNOWLEDGMENT

Work performed under the auspices of the U.S. Department of Energy by the Lawrence Livermore National Laboratory under Contract no. W-7405-ENG-48.

#### REFERENCES

- |  |   |
|--|---|
| <p>Bischoff, K.B., and Levenspiel, O. (1962), "Fluid Dispersion - Generalization and Comparison of Mathematical Models - I", Chem. Eng. Sci., 17, 245-255.</p> <p>Bischoff, K.B.B. (1969), "A Note on Gas Dispersion in Packed Beds," Chem. Eng. Sci. J., 24, 607.</p> <p>Brenner, H. (1962), "The Diffusion Model of Longitudinal Mixing in Beds of Finite Length. Numerical Values," Chem. Eng. Sci., 17, 229.</p> | <p>Coberly, C.A., and Marshall, W.R. (1951), "Temperature Gradients in Gas Streams Flowing through Fixed Granular Beds," Chem. Eng. Prog., 47, 141-150.</p> <p>Deissler, R.G., and Boegli, J.S. (1958), "An Investigation of Effective Thermal Conductivities of Powders in Various Gases," ASME Trans., 1417-1425.</p> <p>Denn, M., Wei, J., Yu W.-C., and Cwiklinski, R. (1982), "Detailed Simulation of a Moving-Bed Gasifier," EPRI Report AP-2576.</p> <p>Dixon, A.G., and Cresswell, D.L. (1979), "Theoretical Prediction of Effective Heat Transfer Parameters in Packed Beds," AIChE J., 25, 663-676.</p> |
|--|---|

- Edwards, M.F., and Richardson, J.F. (1968), "Gas Dispersion in Packed Beds," Chem. Eng. Sci. J., 23, 109-123.
- Field, M.A., Gill, D.W., Morgan, B.B., and Hawksley, P.G.W. (1967), "Combustion of Pulverized Coal," Cheney & Sons Ltd., 322-325.
- Gear, C.W. (1971), "The Automatic Integration of Ordinary Differential Equations," Communication of ACM, 1, 176.
- Govind, R. and Shah, J. (1984), "Modeling and Simulation of an Entrained Flow Coal Gasifier," AIChE J., 3, 79.
- Gunn, R.D. and Whitman, D.L. (1976), "An In Situ Gasification Model (Forward Mode) for Feasibility Studies and Design," Laramie Energy Research Center, Report LERC/RI-76/2.
- Hindmarsh, A.C. (1980), "Two New Initial Value Ordinary Differential Equation Solvers," ACM Newsletter, 15, 10.
- Olbrich, W.E., and Potter, O.E. (1972), "Mass Transfer from the Wall in Small Diameter Packed Beds," Chem. Eng. Sci., 27, 1733-1743.
- Peters, N. (1979) "Premixed Burning in Diffusion Flames - The Flame Zone Model of Libby and Economos," Int. J. Heat Mass Transfer, 22, 691-703.
- Schlunder, E.U. (1978), "Transport Phenomena in Packed Bed Reactors," Ch.4 in Chemical Reaction Engineering-Houston, Luss, D., and Weekend, V., eds., Amer. Chem. Soc., ACS Symposium Series 72, Wash., D.C.
- Sen Gupta, A., and Thodos, G. (1963), "Direct Analogy Between Mass and Heat Transfer to Beds of Spheres," AIChE J., 9, 751.
- Sherwood, T., Pigford, R., and Wilke, C. (1975), Mass Transfer, McGraw-Hill Publish. Co., New York, 129-137.
- Sohrab, S., Ye, Z., and Law, C. (1984), "Theory of Interactive Combustion of Counterflow Premixed Flames," Spring Tech. Mtg. Western States of the Combustion Institute, Boulder, CO, 9.
- Sincovec, R.F. and Madsen, N.K. (1975), "Software for Nonlinear Partial Differential Equations," ACM Transactions on Mathematical Software, 1, 232 .
- Thorsness, C.B., Grens, E.A., and Sherwood, A.E. (1978), "A One-Dimensional Model for In Situ Coal Gasification," Lawrence Livermore National Laboratory, Report UCRL-52523.
- Thorsness, C.B. and Cena, R.J. (1983), "An Underground Coal Gasification Cavity Simulator with Solid Motion," Lawrence Livermore National Laboratory, Report UCRL-89084.
- Thorsness, C.B., and Kang, S-W. (1984), "A Method-Of-Line Approach to Solution of Packed-Bed Flow Problems Related to Underground Coal Gasification Processes," Proc. 10th Annual Underground Coal Gasification Symposium, Williamsburg, VA.
- Thorsness, C.B., and Kang, S-W. (1985), "A General-purpose, Packed-bed Model for Analysis of Underground Coal Gasification Processes," Lawrence Livermore National Laboratory Report (in preparation).
- Wakao, N., and Kaguei, S. (1982), Heat and Mass Transfer in Packed Beds, Gordon and Breach Science Publ., New York.
- Yagi, S., and Kunii, D. (1957), "Studies of Effective Thermal Conductivities in Packed Beds," AIChE J., 3, 373-381.
- Yoon, H., Wei, J., and Denn, M. (1978), "A Model for Moving Bed Gasification Reactors," AIChE J., 2, 885.